

AD-761 646

A STUDY OF DIFFERENT METHODS OF CODING
A CAPPED MODEL

J. Isenberg

Agbabian Associates

Prepared for:

Defense Nuclear Agency

January 1973

DISTRIBUTED BY:

NTIS

National Technical Information Service
U. S. DEPARTMENT OF COMMERCE
5285 Port Royal Road, Springfield Va. 22151



AD 761646

A STUDY OF DIFFERENT METHODS OF CODING A CAPPED MODEL

J. Isenberg

D D C
RECEIVED
JUN 18 1973
C

Prepared by
NATIONAL TECHNICAL
INFORMATION SERVICE
U.S. Department of Commerce
Springfield, MA 01104

Contract No. DNA001-72-C-0045

Prepared for
DEFENSE NUCLEAR AGENCY
Washington, D. C.

AGBABIAN ASSOCIATES
El Segundo, California

Approved for Public Release; Distribution Unlimited

43

DOCUMENT CONTROL DATA - R&D

(Security classification of title, body of abstract and indexing annotation must be entered when the overall report is classified)

1 ORIGINATING ACTIVITY (Corporate author) Agbabian Associates 250 N. Nash Ave. El Segundo, Calif.		2a REPORT SECURITY CLASSIFICATION Unclassified	
		2b GROUP	
3 REPORT TITLE A Study of Different Methods of Coding a Capped Model			
4 DESCRIPTIVE NOTES (Type of report and inclusive dates) Topical Report			
5 AUTHOR(S) (Last name, first name, initial) Isenberg, J.			
6. REPORT DATE October 1972		7a. TOTAL NO. OF PAGES 35	7b. NO. OF REFS 1
8a. CONTRACT OR GRANT NO. DNA001-72-C-0045		9a. ORIGINATOR'S REPORT NUMBER(S) DNA 3067T	
b. PROJECT NO. NWER Code XAXS			
c. Task and Subtask B047		9b. OTHER REPORT NO.(S) (Any other numbers that may be assigned this report) R-7134-2174	
d. Work Unit 45			
10. AVAILABILITY/LIMITATION NOTES Approved for public release; distribution unlimited			
11. SUPPLEMENTARY NOTES		12. SPONSORING MILITARY ACTIVITY Director Defense Nuclear Agency Washington, D.C.	
13. ABSTRACT <p>A study has been made of methods of adapting constitutive equations for granite to numerical computations of wave propagation. The constitutive equations considered are the so-called "capped" model, which incorporates a strain-hardening surface to control dilatancy and a stationary fracture surface. Difficulties have been encountered in some instances when this model has been used for ground shock computations because the model was improperly coded. This report describes two acceptable methods of coding the model and the results of some test cases which will help reveal errors in the future where similar complicated constitutive equations are being coded for the first time.</p>			

14	KEY WORDS	LINK A		LINK B		LINK C	
		ROLE	WT	ROLE	WT	ROLE	WT
Constitutive equations wave propagation							

INSTRUCTIONS

1. ORIGINATING ACTIVITY: Enter the name and address of the contractor, subcontractor, grantee, Department of Defense activity or other organization (*corporate author*) issuing the report.

2a. REPORT SECURITY CLASSIFICATION: Enter the overall security classification of the report. Indicate whether "Restricted Data" is included. Marking is to be in accordance with appropriate security regulations.

2b. GROUP: Automatic downgrading is specified in DoD Directive 5200.10 and Armed Forces Industrial Manual. Enter the group number. Also, when applicable, show that optional markings have been used for Group 3 and Group 4 as authorized.

3. REPORT TITLE: Enter the complete report title in all capital letters. Titles in all cases should be unclassified. If a meaningful title cannot be selected without classification, show title classification in all capitals in parenthesis immediately following the title.

4. DESCRIPTIVE NOTES: If appropriate, enter the type of report, e.g., interim, progress, summary, annual, or final. Give the inclusive dates when a specific reporting period is covered.

5. AUTHOR(S): Enter the name(s) of author(s) as shown on or in the report. Enter last name, first name, middle initial. If military, show rank and branch of service. The name of the principal author is an absolute minimum requirement.

6. REPORT DATE: Enter the date of the report as day, month, year, or month, year. If more than one date appears on the report, use date of publication.

7a. TOTAL NUMBER OF PAGES: The total page count should follow normal pagination procedures, i.e., enter the number of pages containing information.

7b. NUMBER OF REFERENCES: Enter the total number of references cited in the report.

8a. CONTRACT OR GRANT NUMBER: If appropriate, enter the applicable number of the contract or grant under which the report was written.

8b, 8c, & 8d. PROJECT NUMBER: Enter the appropriate military department identification, such as project number, subproject number, system numbers, task number, etc.

9a. ORIGINATOR'S REPORT NUMBER(S): Enter the official report number by which the document will be identified and controlled by the originating activity. This number must be unique to this report.

9b. OTHER REPORT NUMBER(S): If the report has been assigned any other report numbers (*either by the originator or by the sponsor*), also enter this number(s).

10. AVAILABILITY/LIMITATION NOTICES: Enter any limitations on further dissemination of the report, other than those

imposed by security classification, using standard statements such as:

- (1) "Qualified requesters may obtain copies of this report from DDC."
- (2) "Foreign announcement and dissemination of this report by DDC is not authorized."
- (3) "U. S. Government agencies may obtain copies of this report directly from DDC. Other qualified DDC users shall request through _____."
- (4) "U. S. military agencies may obtain copies of this report directly from DDC. Other qualified users shall request through _____."
- (5) "All distribution of this report is controlled. Qualified DDC users shall request through _____."

If the report has been furnished to the Office of Technical Services, Department of Commerce, for sale to the public, indicate this fact and enter the price, if known.

11. SUPPLEMENTARY NOTES: Use for additional explanatory notes.

12. SPONSORING MILITARY ACTIVITY: Enter the name of the departmental project office or laboratory sponsoring (*paying for*) the research and development. Include address.

13. ABSTRACT: Enter an abstract giving a brief and factual summary of the document indicative of the report, even though it may also appear elsewhere in the body of the technical report. If additional space is required, a continuation sheet shall be attached.

It is highly desirable that the abstract of classified reports be unclassified. Each paragraph of the abstract shall end with an indication of the military security classification of the information in the paragraph, represented as (TS), (S), (C), or (U).

There is no limitation on the length of the abstract. However, the suggested length is from 150 to 225 words.

14. KEY WORDS: Key words are technically meaningful terms or short phrases that characterize a report and may be used as index entries for cataloging the report. Key words must be selected so that no security classification is required. Identifiers, such as equipment model designation, trade name, military project code name, geographic location, may be used as key words but will be followed by an indication of technical context. The assignment of links, rules, and weights is optional.



DNA 3067T

R-7134-2174

**A STUDY OF DIFFERENT METHODS OF
CODING A CAPPED MODEL**

J. Isenberg

January 1973

**THIS WORK SPONSORED BY THE DEFENSE NUCLEAR AGENCY
UNDER NWED SUBTASK SB047-45**

Contract No. DNA001-72-C-0045

**Prepared for
DEFENSE NUCLEAR AGENCY
Washington, D. C.**

**AGBABIAN ASSOCIATES
El Segundo, California**

Approved for Public Release; Distribution Unlimited



CONTENTS

<u>Section</u>		<u>Page</u>
1	INTRODUCTION	1
2	CAPPED MODEL FOR PILE DRIVER GRANITE AND WAYS OF CODING IT	2
	General Equations	2
	Some Problem Areas in Coding Models of This Type	11
3	APPLICATION OF THE CAPPED MODEL IN TWO EXERCISES	15
	Split-Hopkinson Bar Calculation	15
	Stress/Strain Exercises	26
	Subdividing Strain Increments (Splitting)	26
	Iterative Techniques	26
4	SUMMARY AND CONCLUSIONS	32
	REFERENCES	33
 <u>Appendix</u>		
A	METHODS OF CODING THE CAPPED MODEL . .	A-1



ILLUSTRATIONS

<u>Figure</u>		<u>Page</u>
2-1	Fracture Surface and Caps Corresponding to Values of Cap Parameters	5
2-2	Method of Correcting Final Stress State From a Trial State	8
2-3	Regions of Stress Space	13
3-1	Cap Model Test Problem	16
3-2	Stress Path for an Element in Center of Granite on Centerline in Split-Hopkinson Bar Computation	17
3-3	Stress Paths in Stress/Strain Exercises .	19
3-4	Axial Stress at Center of Granite on Centerline	20
3-5	Radial Stress at Center of Specimen on Centerline	21
3-6	Radial Stress Midway Between Centerline and Surface at Weighbar Interface	22
3-7	Axial Stress at Center of the Specimen vs Radius at 50 μ sec	23
3-8	Radial Stress at Center of the Specimen vs Radius at 50 μ sec	24
3-9	Stress Points at Center of Specimen on Centerline at Selected Instants of Time as Computed by Group 1	25
3-10	Automatic Splitting	31



TABLES

<u>Table</u>		<u>Page</u>
3-1	Prescribed Strains for Stress/Strain Exercises	18
3-2	Stress States Corresponding to Strain Paths in Table 3-1	27
3-3	Value of Hardening Parameter for Path 4 (With Cap) Obtained by Group 2 for Different Amounts of Splitting	28
3-4	Value of Axial Stress (σ_1) for Path 4 (With Cap) Obtained with Different Amounts of Splitting by Three Groups. Difference Between Groups 1 and 2 for $\Delta E/1000$ is Attributed to Different Definition of Strain Variables.	29
3-5	Value of Radial Stress (σ_2) for Path 4 (With Cap) Obtained with Different Amounts of Splitting by Three Groups . .	30



SECTION 1

INTRODUCTION

This report shows how constitutive equations for elastic/strain-hardening materials are formulated for computer programs which calculate wave propagation. The constitutive equations considered here are for Pile Driver granite and were developed by I. Sandler of Paul Weidlinger Consulting Engineer. (Reference 1)

Prior to performing calculations of the Pile Driver event, preliminary calculations were made by several groups to investigate whether there is agreement among various computer codes. The preliminary calculations involve wave propagation for which the input, geometry, material properties, finite difference mesh size and integration time step were specified by the Defense Nuclear Agency (DNA) project officer. Although the calculations represent dynamic loading in a split-Hopkinson Bar testing device, no reference is made to any physical tests. The split-Hopkinson Bar was thought merely to be a useful configuration within which codes can be compared. Comparison among the results of the various preliminary calculations reveals some agreement and some disagreement. A study conducted by Agbabian Associates indicated that part of the differences among the results of the preliminary calculations was due to different methods of coding the constitutive equations. When each of the methods was suitably refined, however, all gave comparable results.

This report documents the methods of coding the capped model which were used during the investigation. The exercises which were performed and results which were found to be acceptable are also discussed.



SECTION 2

CAPPED MODEL FOR PILE DRIVER GRANITE
AND WAYS OF CODING IT

GENERAL EQUATIONS

The model consists of an ideally plastic modified Drucker-Prager yield criterion,

$$f_1(J_1, \sqrt{J_2}) = 0 \dots \dots \dots (2-1)$$

and a cap.

$$f_2(J_1, \sqrt{J_2}, L) = 0 \dots \dots \dots (2-2)$$

where J_1 is the first stress invariant, J_2 is the second invariant of the stress deviators, and L is a given function of the stress-strain history of the rock. Constant bulk and shear moduli are used. The plastic potential flow rule is used to determine plastic strain rates on both f_1 and f_2 .

Yield Functions--Fracture Surface and Cap

The failure criterion f_1 is given by

$$f_1 = \begin{cases} \sqrt{J_2} - \left\{ A \left[1 - \left(1 - \frac{J_1}{B} \right)^2 \right] + C \right\} \leq 0 & \text{for } J_1 < B \\ \sqrt{J_2} - (A + C) \leq 0 & \text{for } J_1 \geq B \end{cases} \quad (2-3)$$

where

$$A = 150 \text{ ksi}$$

$$B = 1000 \text{ ksi}$$

$$C = 3 \text{ ksi}$$



The cap, which is elliptical and tangent to the failure envelope at their point of intersection, is given by

$$f_2 = (J_1 - v)^2 + R^2(J_2' - Q) = 0 \dots\dots\dots (2-4)$$

in which

$$v = L + R^2 X(L) X'(L) \dots\dots\dots (2-5)$$

$$Q = [X(L)]^2 \{1 + R^2 [X'(L)]^2\} \dots\dots\dots (2-6)$$

and

$$X(L) = \begin{cases} A \left[1 - \left(1 - \frac{L}{B} \right)^2 \right] + C & L \leq B \\ A + C & L > B \end{cases} \dots\dots\dots (2-7a)$$

$$X'(L) = \begin{cases} \frac{2A}{B} \left(1 - \frac{L}{B} \right) & L \leq B \\ 0 & L > B \end{cases} \dots\dots\dots (2-7b)$$

The hardening parameter, L , is

$$L = \int_0^t g(J_1, \sqrt{J_2'}) \sqrt{\dot{i}_2^P} dt \dots\dots\dots (2-8)$$

where

$$g = W \left[1 - \frac{\sqrt{J_2'}}{\sqrt{J_2' - f_1}} \right]^2 \dots\dots\dots (2-9)$$

$$\dot{i}_2^P = (\dot{\epsilon}_1^P)^2 + (\dot{\epsilon}_2^P)^2 + (\dot{\epsilon}_3^P)^2 \dots\dots\dots (2-10)$$



The material coefficients R and W are

$$R = 3.0$$

$$W = 10^7 \text{ ksi}$$

The fracture surface and typical caps are illustrated in Figure 2-1.

Bulk and Shear Moduli

The bulk shear modulus B and shear modulus μ are assumed to be constant

$$B = 7000 \text{ ksi}$$

$$\mu = 3000 \text{ ksi}$$

Incremental Stress/Strain Relationship

The incremental stress is related to the elastic component of strain by the expression

$$d\sigma_{ij} = \left(B - \frac{2}{3} \mu \right) \left(d\epsilon_{kk}^e \right) \delta_{ij} + 2\mu \left(d\epsilon_{ij}^e \right) \dots \dots \dots (2-11)$$

where

$$d\epsilon_{ij}^e = d\epsilon_{ij} - d\epsilon_{ij}^P \dots \dots \dots (2-12)$$

and the plastic strain-increment $\left(d\epsilon_{ij}^P \right)$ is defined by

$$d\epsilon_{ij}^P = \Lambda \frac{\partial f}{\partial \sigma_{ij}} \dots \dots \dots (2-13)$$



STRAIN PATH 3

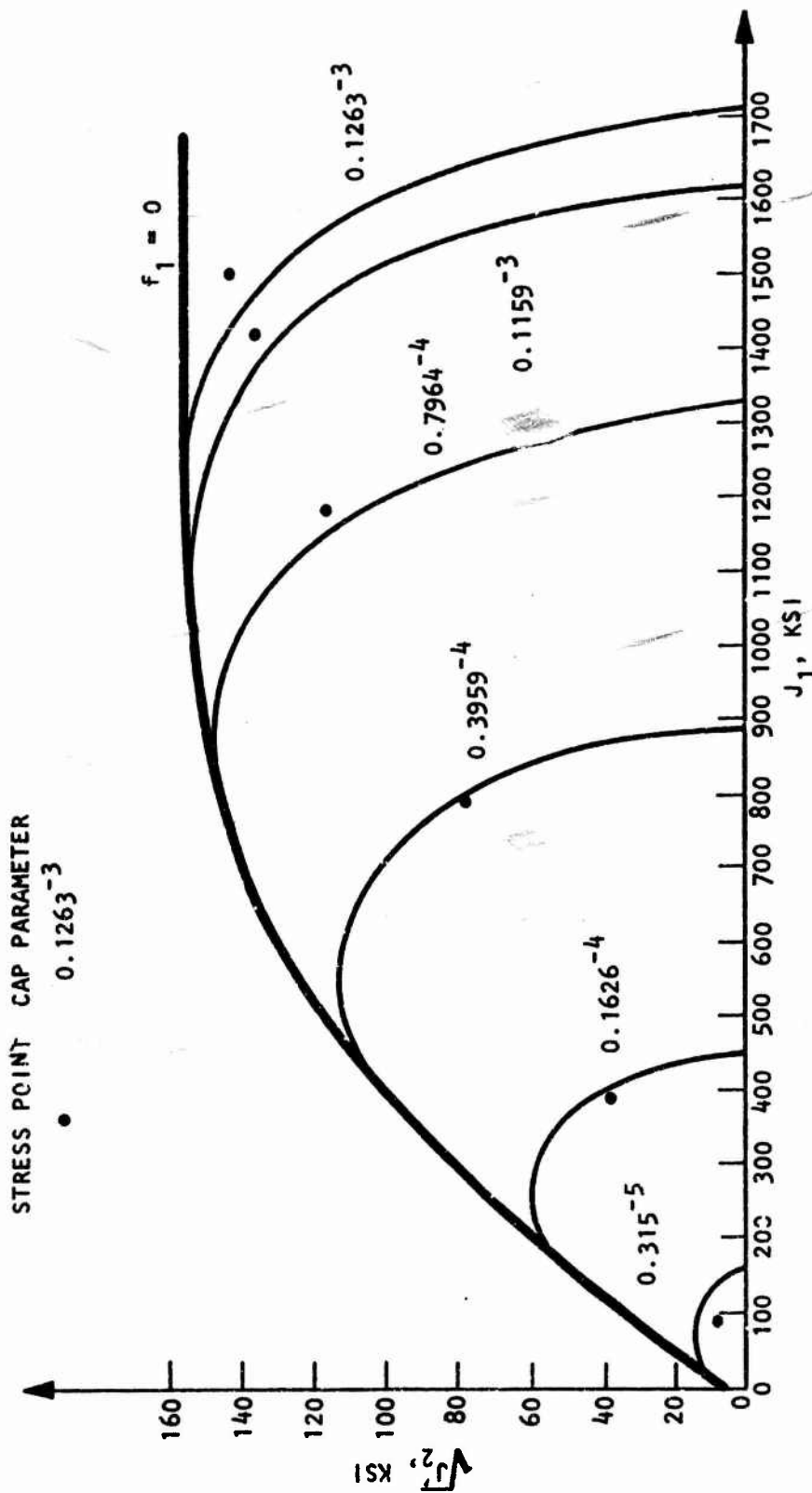


FIGURE 2-1. FRACTURE SURFACE AND CAPS CORRESPONDING TO VALUES OF CAP PARAMETERS



All methods of coding the associated, plastic potential flow rule begin with these statements. Thus

$$d\sigma_{ij} = \lambda \left(d\epsilon_{kk} - \lambda \frac{\partial f}{\partial \sigma_{kk}} \right) \delta_{ij} + 2\mu \left(d\epsilon_{ij} - \lambda \frac{\partial f}{\partial \sigma_{ij}} \right) \dots \dots \dots (2-14)$$

or, in terms of stress invariants,

$$dJ_1 = 3K \left(d\epsilon_{kk} - 3\lambda \frac{\partial f}{\partial J_1} \right) \dots \dots \dots (2-15a)$$

and

$$d\sqrt{J_2'} = \frac{\mu}{\sqrt{J_2'}} \sigma_{ij}' \left(d\epsilon_{ij}' - \lambda \frac{\partial f}{\partial \sigma_{ij}'} \right) \dots \dots \dots (2-15b)$$

where primed quantities denote deviatoric components of stress and strain.

The final stress state, represented by

$$\left(\sigma_{ij} \right)_{new} = \left(\sigma_{ij} \right)_{old} + d\sigma_{ij} \dots \dots \dots (2-16)$$

or

$$\left(J_1 \right)_{new} = \left(J_1 \right)_{old} + dJ_1 \dots \dots \dots (2-17a)$$

$$\left(\sqrt{J_2'} \right)_{new} = \left(\sqrt{J_2'} \right)_{old} + d\sqrt{J_2'} \dots \dots \dots (2-17b)$$

must lie on the curve.*

*The present example is most easily illustrated with a perfectly plastic material. Modifications for a work hardening material are discussed at the end of the chapter.



$$f(\sigma_{ij}) = 0 \dots\dots\dots (2-18a)$$

or

$$f(\sqrt{J_2}, J_1) = 0 \dots\dots\dots (2-18b)$$

The mathematical statement of this constraint, used by all contributors to the present exercise, is

$$df = \frac{\partial f}{\partial \sigma_{ij}} d\sigma_{ij} = 0 \dots\dots\dots (2-19a)$$

or

$$df = \frac{\partial f}{\partial J_1} dJ_1 + \frac{\partial f}{\partial \sqrt{J_2}} d\sqrt{J_2} = 0 \dots\dots\dots (2-19b)$$

At this point, two different approaches are used to obtain the states of stress and plastic strain. The first approach to be described is referred to as Method A and is used by several groups engaged in ground shock calculation. The subscript *t* is used to indicate a trial or temporary state which lies in the forbidden region outside $f = 0$ as indicated in Figure 2-2. The increment in stress or stress invariant from the old, equilibrium state to the trial state is denoted by $(d\sigma_{ij})_t$, $(dJ_1)_t$ and $(d\sqrt{J_2})_t$.

Equations 2-15a and -15b may be rewritten as follows:

$$dJ_1 = (dJ_1)_t - 9KA f_{kk} \dots\dots\dots (2-20a)$$

$$d\sqrt{J_2} = (d\sqrt{J_2})_t - 2GA \sigma'_{ij} f'_{ij} \dots\dots\dots (2-20b)$$

where

$$f_{kk} = \frac{\partial f}{\partial \sigma_{kk}} = f_I$$

$$f'_{ij} = \frac{\partial f}{\partial \sigma'_{ij}} = \frac{\partial f}{\partial \sqrt{J_2}} \frac{\partial \sqrt{J_2}}{\partial \sigma'_{ij}} = f_{II} \left(\frac{\sigma'_{ij}}{2\sqrt{J_2}} \right)$$

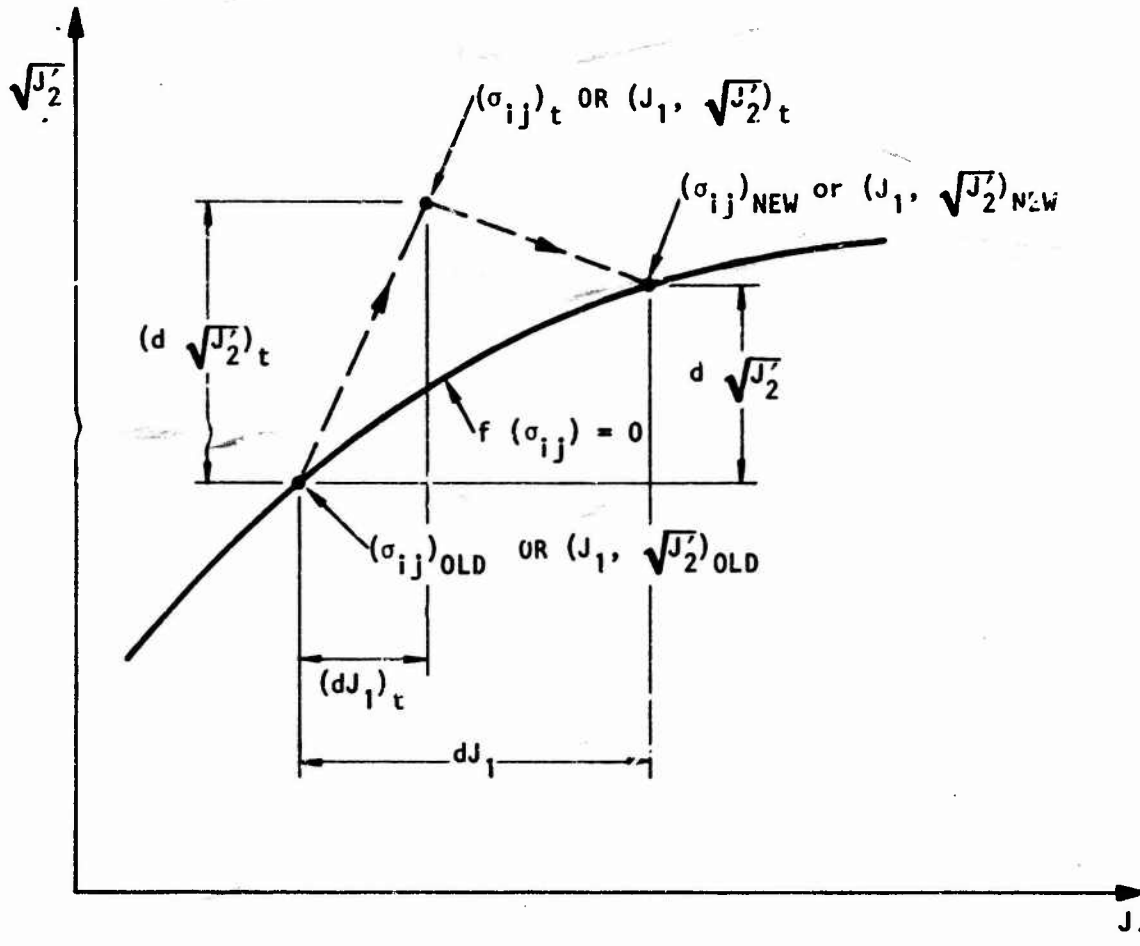


FIGURE 2-2. METHOD OF CORRECTING FINAL STRESS STATE FROM A TRIAL STATE



Substituting Equations 2-20a and -20b into 2-19b

$$f_I \left[\left(dJ_1 \right)_t - 9K\Lambda f_I \right] + f_{II} \left[\left(d\sqrt{J_2} \right)_t - \frac{\mu\Lambda\sigma_{ij}^i\sigma_{ij}^i f_{II}}{2\sqrt{J_2}^i\sqrt{J_2}^i} \right] = 0 \dots (2-21)$$

Equation 2-21 may also be expressed by

$$9K\Lambda f_I^2 + \mu\Lambda f_{II}^2 = f_I \left(dJ_1 \right)_t + f_{II} \left(d\sqrt{J_2} \right)_t \dots (2-22)$$

The expression on the right-hand side of Equation 2-22 is considered to be equal to the difference between the trial state and the surface $f = 0$. Thus

$$f \left[\left(J_1 \right)_t, \left(\sqrt{J_2} \right)_t \right] \geq 0 = f_I \left(dJ_1 \right)_t + f_{II} \left(d\sqrt{J_2} \right)_t \dots (2-23)$$

Λ is then computed from the expression

$$\Lambda = \frac{f \left[\left(J_1 \right)_t, \left(\sqrt{J_2} \right)_t \right]}{9Kf_I^2 + \mu f_{II}^2} \dots (2-24)$$

The plastic strain increments can be found by substituting this value of Λ into Equation 2-13. The increments in J_1 and $\sqrt{J_2}$ can be found by substituting Λ into Equations 2-20a and -20b.

In an alternative approach, referred to as Method B, Equation 2-14 is substituted into Equation 2-19a as follows.

$$f_{ij} (\lambda d\epsilon_{kk} - \Lambda f_{\ell\ell}) \delta_{ij} + 2\mu f_{ij} (d\epsilon_{ij} - \Lambda f_{ij}) = 0 \dots (2-25)$$



and Λ is computed from the expression

$$\Lambda = \frac{\lambda(d\epsilon_{kk})^f_{\ell\ell} + 2\mu d\epsilon_{ij} f_{ij}}{\lambda f_{kk} f_{\ell\ell} + 2\mu f_{ij} f_{ij}} \dots \dots \dots (2-26)$$

If the stress point lines on the capped portion of the yield surface, Equations 2-24 and 2-26 must be modified to account for motion of the cap. In the present model, this modification is as follows.

Method A

$$\Lambda = \frac{f[(J_1)_t, (\sqrt{J_2})_t]}{9kf_1^2 + \mu f_{11}^2 + g \frac{\partial f}{\partial L} \sqrt{f_{11}^2 + f_{22}^2 + f_{33}^2}} \dots \dots \dots (2-24a)$$

Method B

$$\Lambda = \frac{\lambda(d\epsilon_{\ell\ell}) f_{\ell\ell} + 2\mu d\epsilon_{ij} f_{ij}}{\lambda f_{\ell\ell} f_{\ell\ell} + 2\mu f_{ij} + g \frac{\partial f}{\partial L} \sqrt{f_{11}^2 + f_{22}^2 + f_{33}^2}} \dots \dots \dots (2-26a)$$

The values of Λ obtained by Equations 2-24 and 2-26 are the same if the derivatives of f with respect to stress and stress invariants are the same. The derivatives differ if the stresses used to evaluate them differ. Some groups use the trial stress invariants $(J_1)_t, (\sqrt{J_2})_t$ to evaluate the derivatives. Other groups use the stresses at the previous state $(\sigma_{ij})_{old}$ to evaluate the derivatives. If the difference between the trial and the old states is large enough, or if f is a sufficiently nonlinear function of its arguments, then noticeable differences between the two approaches will develop. Appreciable differences do not develop if either of the above conditions is absent. In some of the examples given below, the trial and the old states are kept close by the device of subdividing the strain increment into many smaller increments.



SOME PROBLEM AREAS IN CODING MODELS OF THIS TYPE

The main difficulties in coding this model arise because important parameters of the model are implicit functions of stress and plastic strain quantities. Before the new stresses and plastic strains can be computed, functions which depend on them must first be evaluated. The dilemma is relatively easily resolved when the function f corresponds to the fracture surface because the values of $\partial f / \partial \sigma_{ij}$ do not usually change rapidly with changes in σ_{ij} . Almost any technique involving iteration or subdivision of the strain increments leads to a correct answer so long as enough steps are taken from $(\sigma_{ij})_{old}$ to $(\sigma_{ij})_{new}$. In fact, if the slope of the fracture surface is constant, an exact relationship between the trial and final stress states can be found in closed form as follows. Assuming the fracture criterion be given by

$$f_1 = \sqrt{J_2^t} - \alpha J_1 - C \leq 0 \quad \dots \dots \dots (2-27)$$

The associated, plastic potential flow rule leads to

$$(J_1)_{new} = J_{1t} \left(\frac{G}{9K\alpha^2 + G} \right) + \left(\sqrt{J_{2t}^t} - C \right) \left(\frac{9K\alpha}{9K\alpha^2 + G} \right) \quad (2-28)$$

$$\left(\sqrt{J_2^t} \right)_{new} = \sqrt{J_{2t}^t} - G \frac{\sqrt{J_{2t}^t} - C - \alpha J_{1t}}{9K\alpha^2 + G} \quad \dots \dots \dots (2-29)$$

The strain hardening or cap portion of the model is much more difficult to code. The rate at which convergence to the right answer proceeds depends greatly on the technique of iteration or of subdividing the strain increment.

Two basic approaches were used for finding the correct cap and stress point in the examples reported below. One approach is to rely completely on an iterative technique. Such an approach hopes to accommodate $d\sigma_{ij}$ which are of the same order as $(\sigma_{ij})_{old}$ and

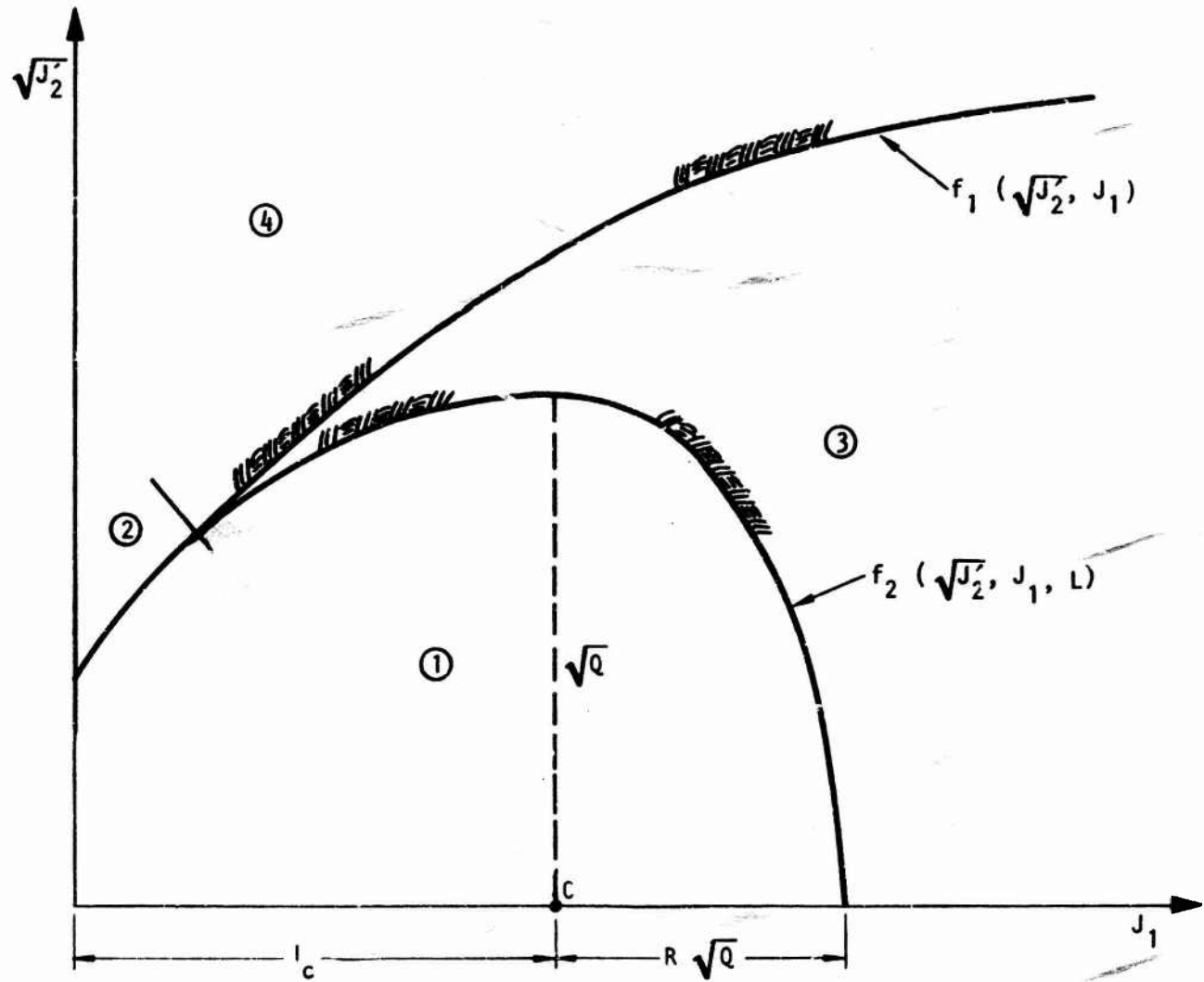


correspondingly large changes in the cap parameter. It is argued that this procedure is consistent with the finite changes in stresses and velocities which occur in time-marching computations of shock wave propagation.

An alternative approach is to subdivide or split the strain increment into a series of subincrements in which $d\sigma_{ij}$ is much smaller than $(\sigma_{ij})_{old}$. This has the effect of enabling equations such as Equation 2-19 to be regarded as linear difference equations. The derivatives $\partial f/\partial \sigma_{ij}$, etc. are still implicit functions of plastic strain, and hence an iterative scheme such as a Newton-Raphson technique or a modified Euler approach which averages the matrix of generalized stress/strain coefficients is still required. It is argued that this is consistent with the assumption that the stress/strain rules being coded are continuous in slope and function value. One difficulty which both methods must overcome is illustrated in Figure 2-3, which shows how a trial stress increment may penetrate both the cap and the fracture surface. The questions which the code must resolve automatically are

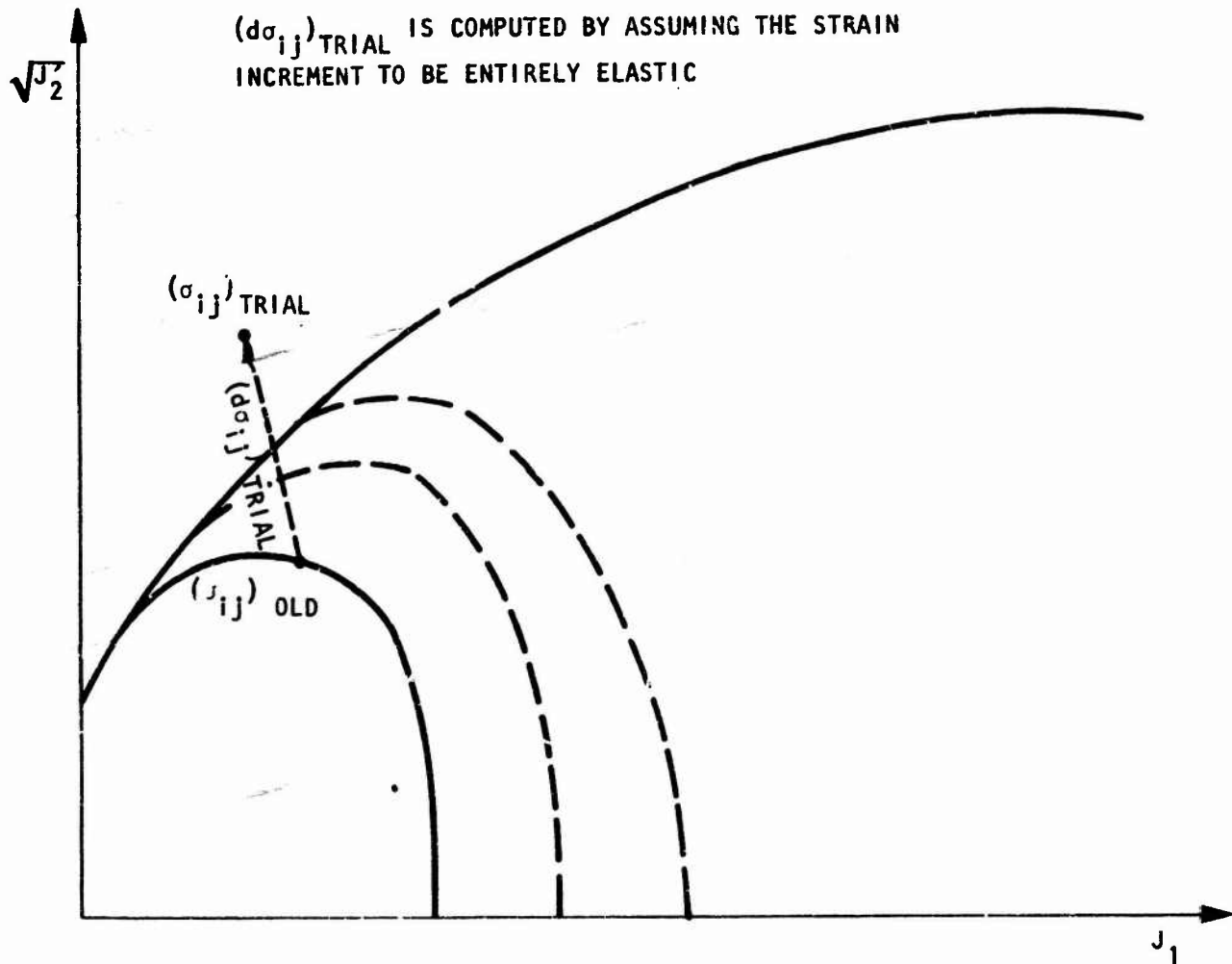
- a. Which surface should the stress point be on?
- b. Which point of the surface selected in a should the stress point be on?

These questions are discussed further in Appendix A.



(a) REGION OF $J_1/\sqrt{J_2}$ PLANE INTO WHICH TRIAL STRESS STATES MAY FALL

FIGURE 2-3. REGIONS OF STRESS SPACE



- (b) A POSSIBLE SITUATION WHERE THE CODE MUST DECIDE IN WHICH REGION THE STRESS POINT ULTIMATELY SHOULD BE

FIGURE 2-3. (CONTINUED)



SECTION 3

APPLICATION OF THE CAPPED MODEL IN TWO EXERCISES

The results of two exercises are reported below. The first exercise represents a split-Hopkinson bar apparatus with a granite specimen, whose constitutive relations are governed by the capped model, inserted between steel bars. Figure 3-1 shows the dimensions, zone size, time step and properties. The stress path followed by elements in the center of the granite is illustrated in Figure 3-2. Since most of the zones undergoing plasticity are in a state of approximately uniaxial stress only a small part of the capped model is exercised in the computation.

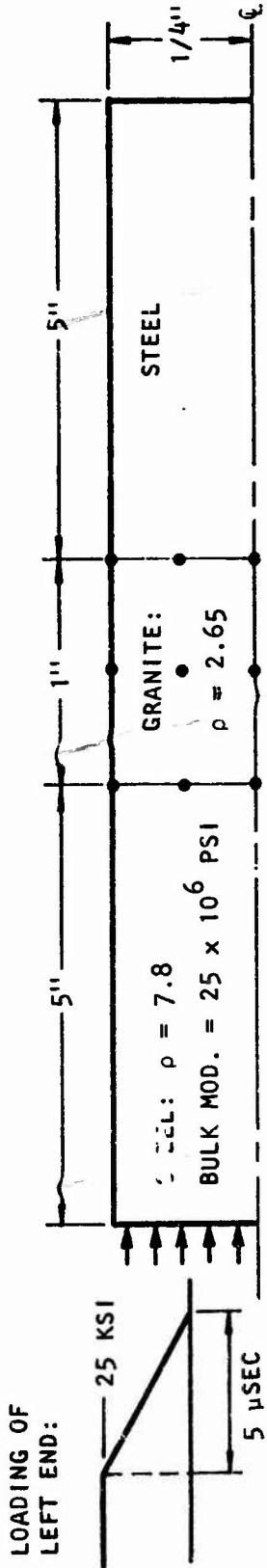
To expand the scope of the present investigation, further exercises were performed in which five different stress paths are followed. The paths are specified by the combinations of principal strains and are listed in Table 3-1. The paths in $\sqrt{J_2}/J_1$ plane which an elastic material would follow when subjected to these strains are shown in Figure 3-3.

SPLIT-HOPKINSON BAR CALCULATION

Some of the differences in the split-Hopkinson bar calculation which prompted the present study are shown in Figure 3-4 through 3-9. Group 1 correctly coded the model using Method A as described above. Group 2 correctly coded the model using Method B. Besides using a different method to compute Λ , the main differences in coding the material model were:

- a. In evaluating functions of stresses, Group 1 used the trial state stresses (σ_t) whereas Group 2 used the previous state stresses (σ_{old}).
- b. Group 1 subdivided the strain increments into smaller subincrements whereas Group 2 used the full increment.

Thus, although both methods are in principle correct, significant differences occur. No exact solution is available, so that it is impossible to say with assurance that one computation is better than the other. However, due to splitting the strain-increment, the results obtained by Group 1 have a better chance of being more accurate. Due to performing a greater number of operations in the material property subroutines of the computer program, the calculation performed by Group 1 is also more expensive than it would be if splitting were omitted.



SHEAR MOD.

= 11.62 x 10⁶ PSI
(LINEAR ELASTIC)

ZONING: 50 x 6 ZONING: 10 x 6 ZONING: 50 x 6
(ΔX = 0.1" (ΔX = 0.1" ΔR = 0.04167")
ΔR = 0.04167")

1. RUN PROBLEM FOR 500* TIME STEPS, Δt = 0.1 μSEC
2. OBTAIN OUTPUT AT STATIONS NOTED ABOVE IN GRANITE (·). OUTPUT OF INTEREST IS DISPLACEMENTS (ΔX, ΔR), VELOCITIES (ẋ, Ṙ), AND STRESSES (σ_X, σ_R).

*SHOULD GIVE 4-5 REVERBERATIONS ("ROUND TRIPS") IN GRANITE

FIGURE 3-1. CAP MODEL TEST PROBLEM

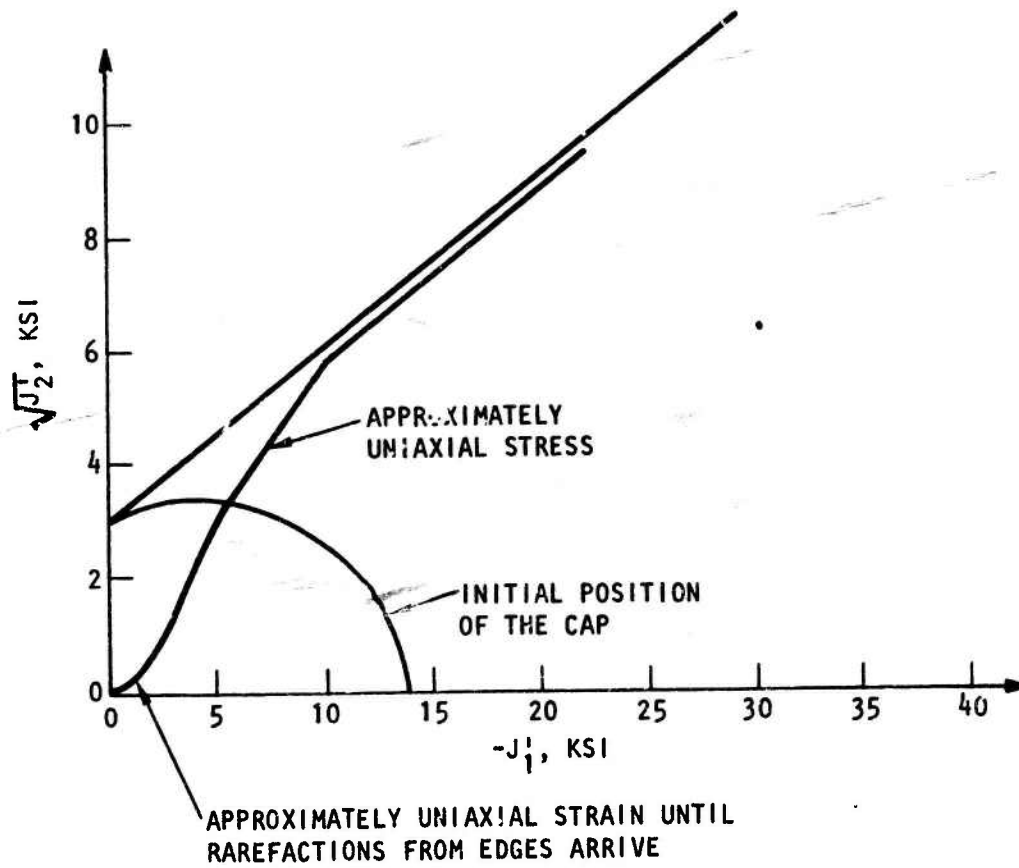


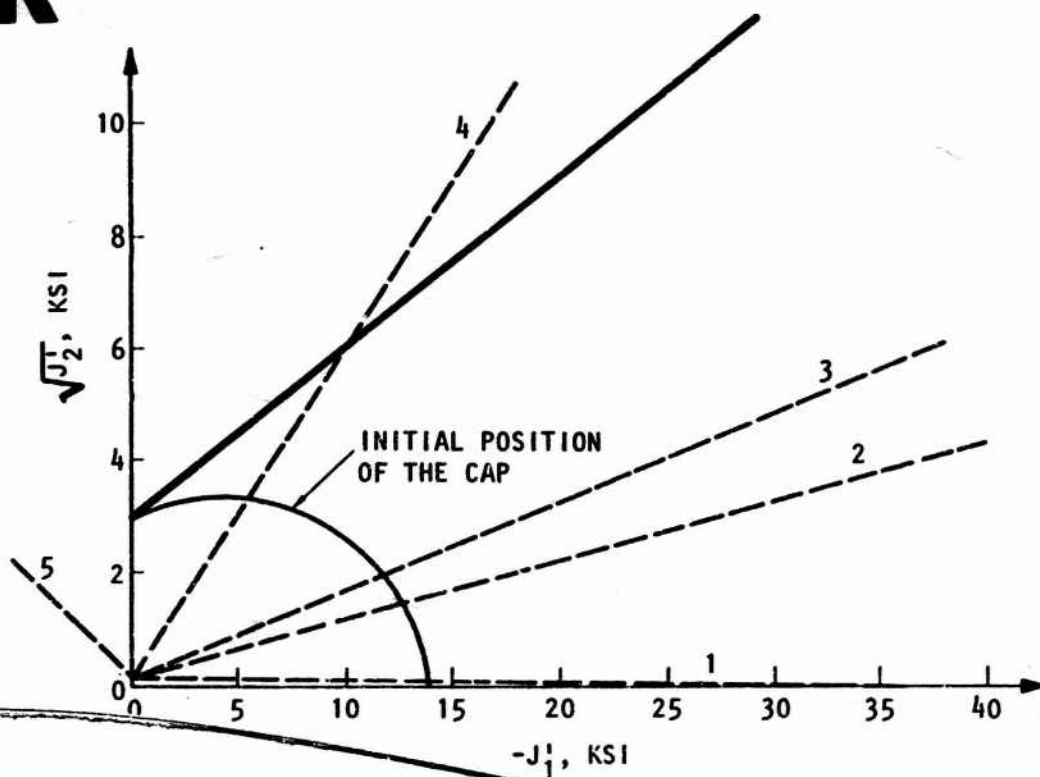
FIGURE 3-2. STRESS PATH FOR AN ELEMENT IN CENTER OF GRANITE ON CENTERLINE IN SPLIT-HOPKINSON BAR COMPUTATION



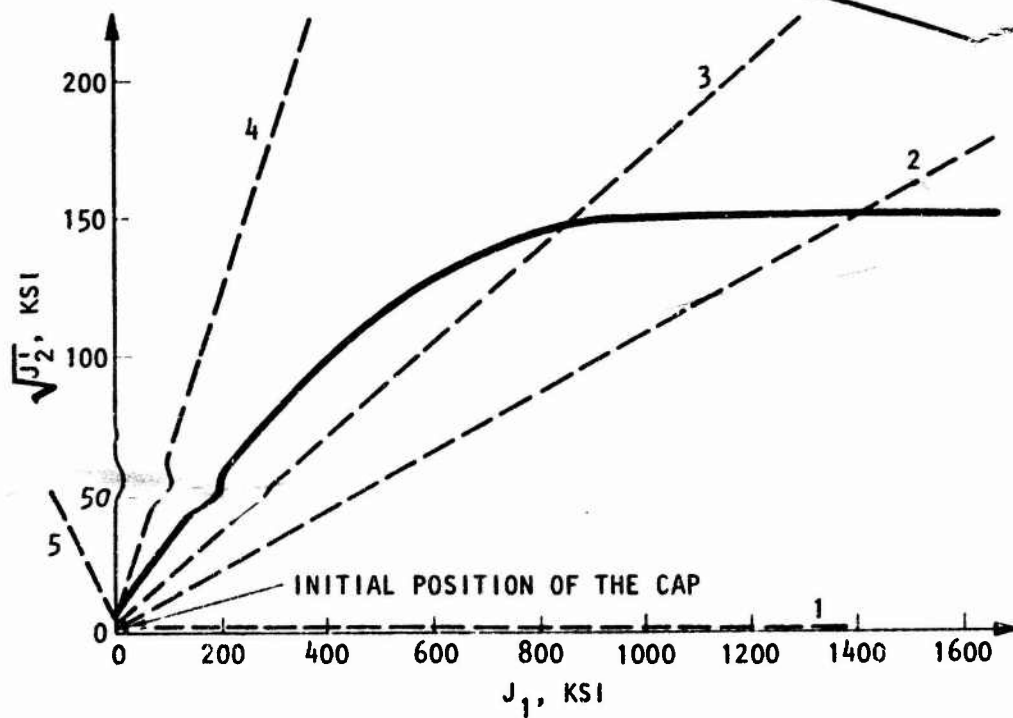
TABLE 3-1. PRESCRIBED STRAINS FOR STRESS/STRAIN EXERCISES

Path	Step	ϵ_{11}	$\epsilon_{22} = \epsilon_{33} = \eta\epsilon_{11}$
1 ($\eta = 1$)	a	2.38×10^{-4}	2.38×10^{-4}
	b	2.38×10^{-3}	2.38×10^{-3}
	c	2.38×10^{-2}	2.38×10^{-2}
2 ($\eta = 0.354$)	a	3.2×10^{-4}	1.13×10^{-4}
	b	3.2×10^{-3}	$.13 \times 10^{-3}$
	c	3.2×10^{-2}	1.13×10^{-2}
	d	6.4×10^{-2}	2.26×10^{-2}
3 ($\eta = 0.179$)	a	3.5×10^{-4}	0.626×10^{-4}
	b	3.5×10^{-3}	0.626×10^{-3}
	c	2.8×10^{-2}	0.501×10^{-2}
	d	5.6×10^{-2}	1.00×10^{-2}
4 ($\eta = -0.212$)	a	4.13×10^{-4}	-0.875×10^{-4}
	b	6.61×10^{-3}	-1.4×10^{-3}
	c	1.15×10^{-2}	-2.45×10^{-3}
	d	3.31×10^{-2}	-7.01×10^{-3}
5 ($\eta = 0.702$)	a	-4.96×10^{-5}	-3.48×10^{-5}
	b	-7.95×10^{-4}	-5.57×10^{-4}

Positive sign indicates compressive strain.



(a) APPROXIMATE STRESS PATHS FOR STRESS/STRAIN EXERCISES (NEW ORIGIN)



(b) FRACTURE CRITERION, CAP AND ELASTIC PATHS (OVERALL VIEW)

FIGURE 3-3. STRESS PATHS IN STRESS/STRAIN EXERCISES

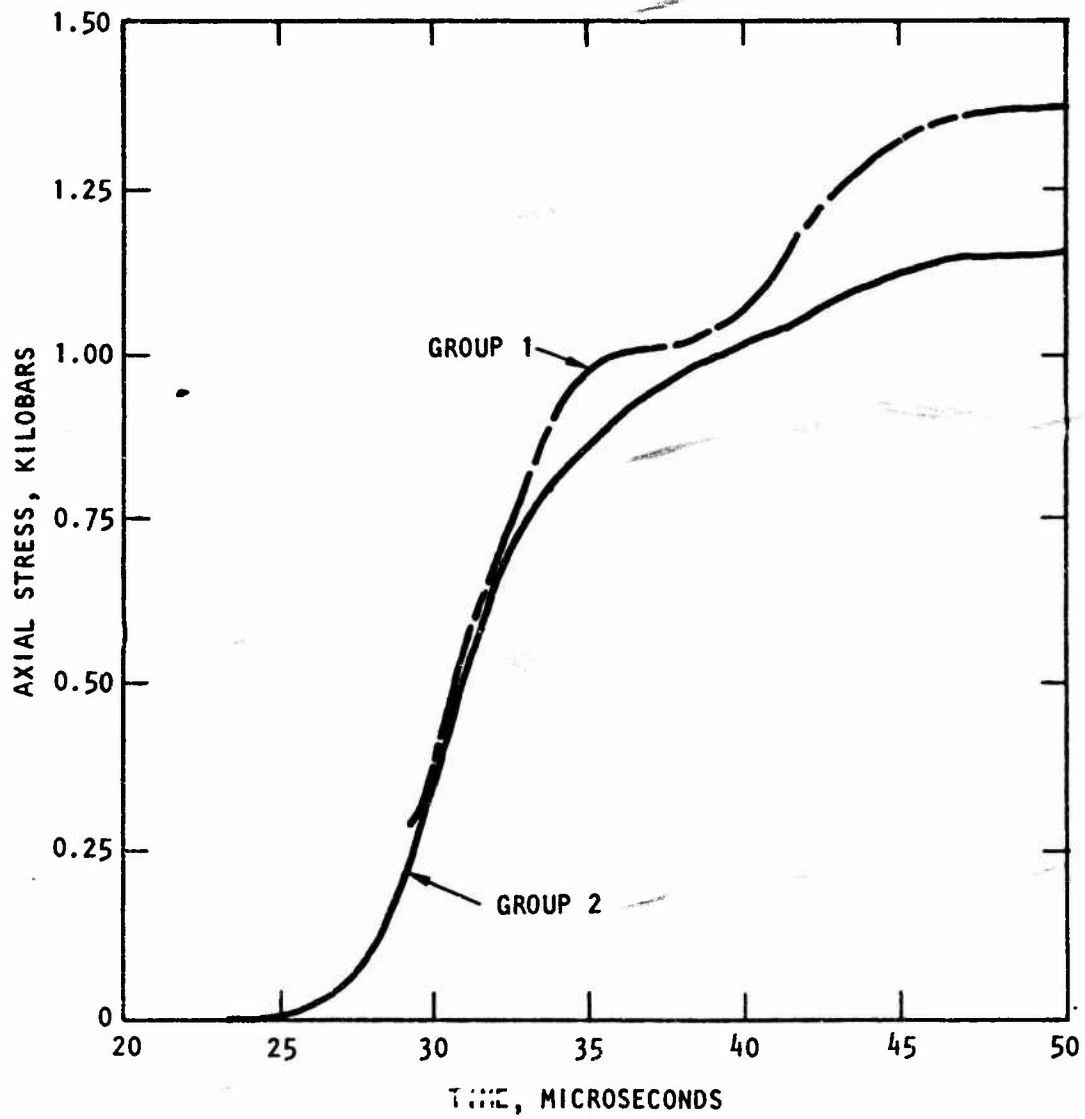


FIGURE 3-4. AXIAL STRESS AT CENTER OF GRANITE ON CENTERLINE

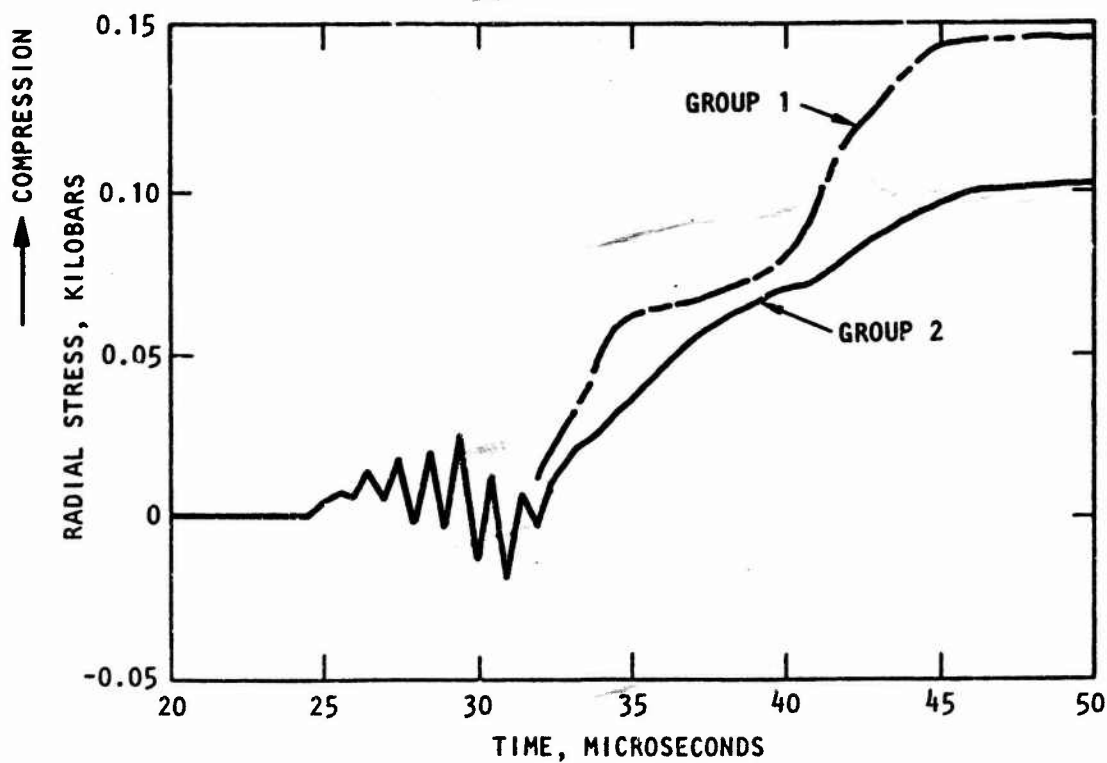


FIGURE 3-5. RADIAL STRESS AT CENTER OF SPECIMEN ON CENTERLINE

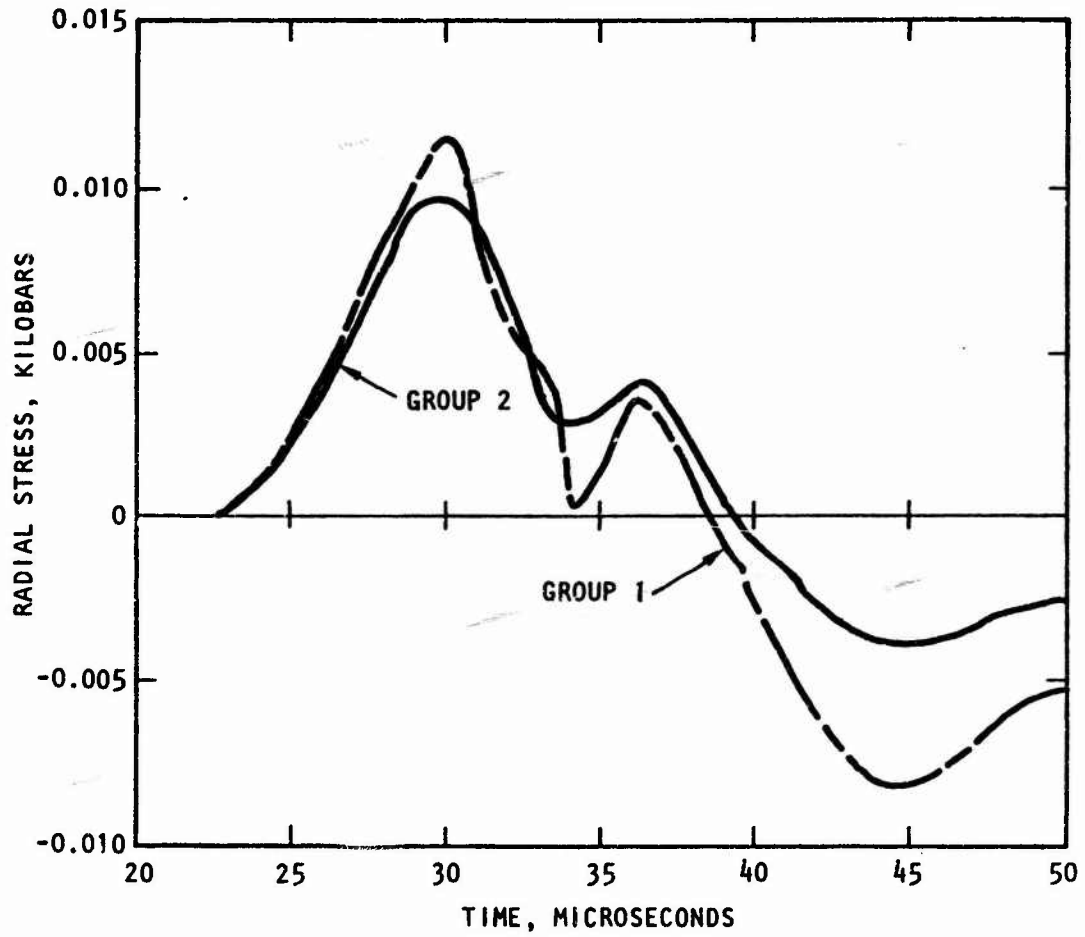


FIGURE 3-6. RADIAL STRESS MIDWAY BETWEEN CENTERLINE AND SURFACE AT WELDBAR INTERFACE

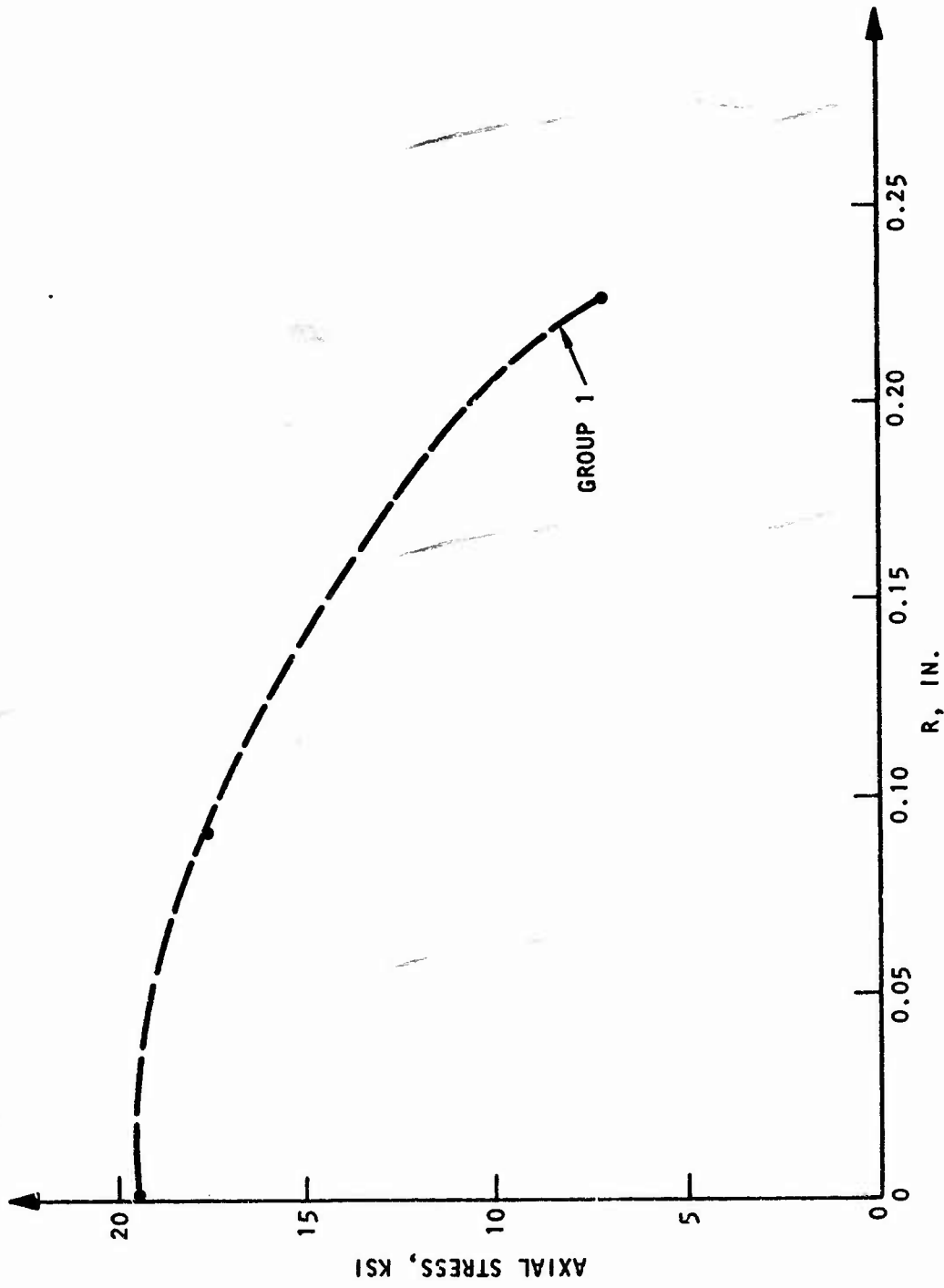


FIGURE 3-7. AXIAL STRESS AT CENTER OF THE SPECIMEN VS RADIUS AT 50 μ SEC

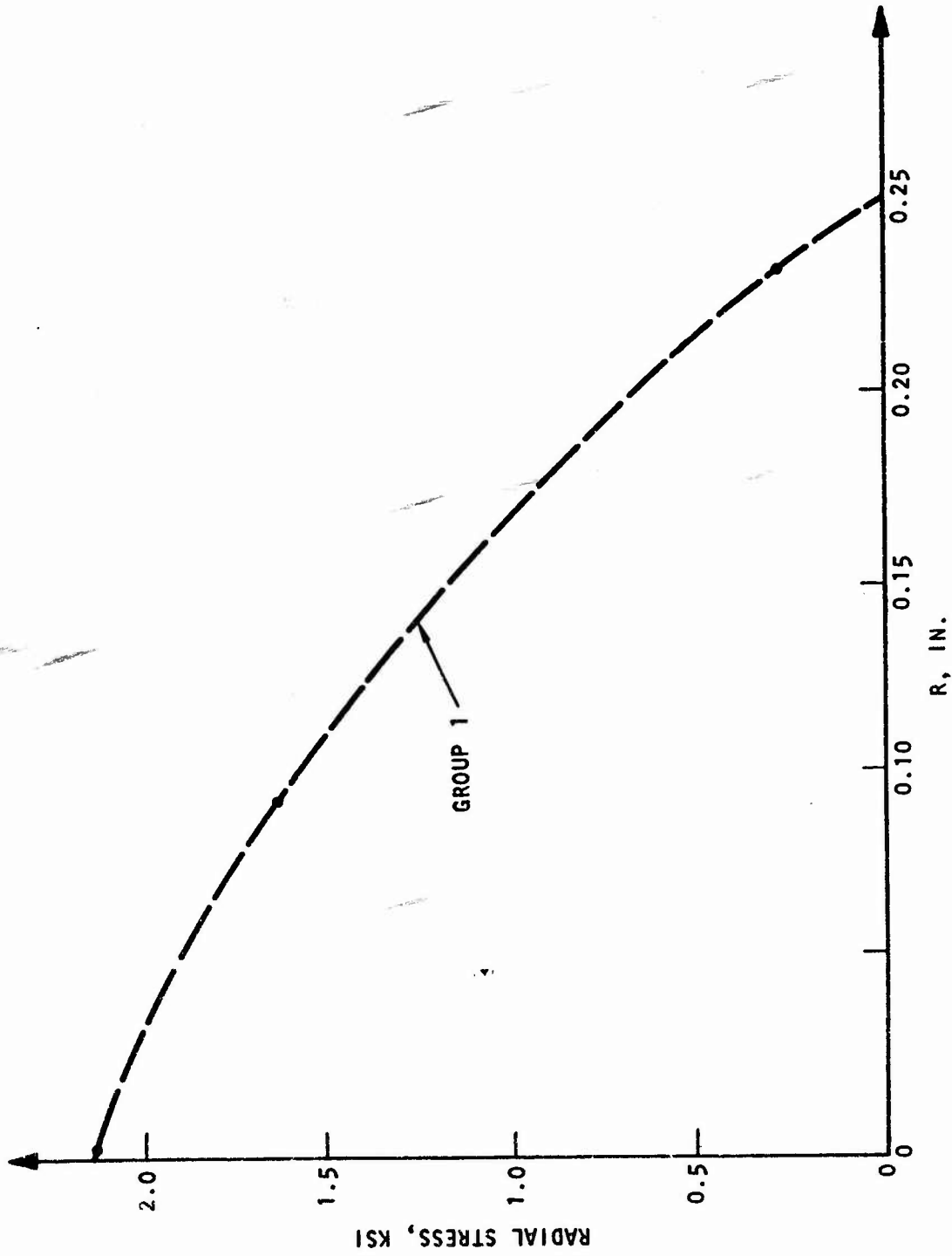


FIGURE 3-8. RADIAL STRESS AT CENTER OF THE SPECIMEN VS RADIUS AT 50 μ SEC

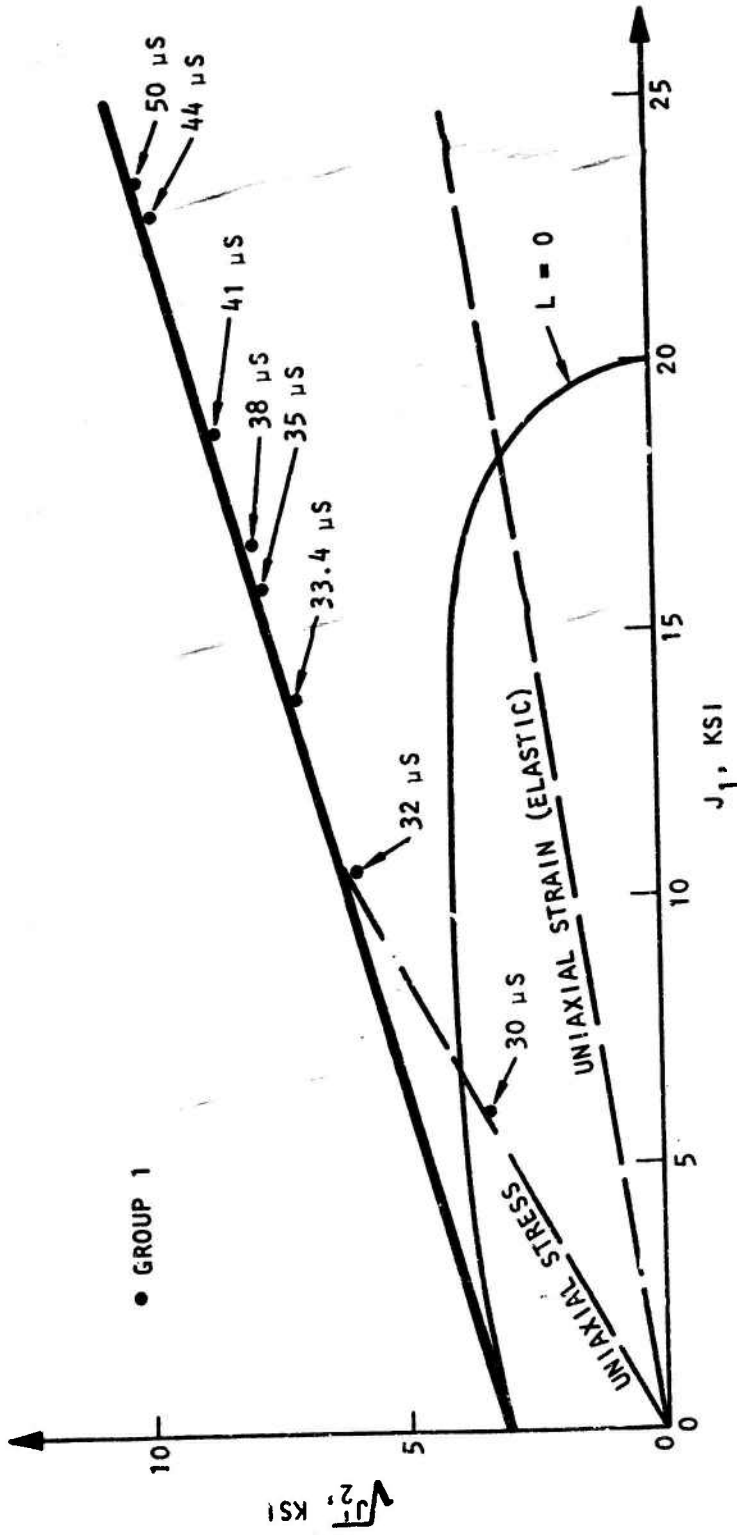


FIGURE 3-9. STRESS POINTS AT CENTER OF SPECIMEN ON CENTERLINE AT SELECTED INSTANTS OF TIME AS COMPUTED BY GROUP 1



STRESS/STRAIN EXERCISES

To provide a basis for comparing various methods of coding the capped model, a series of example problems involving prescribed strain paths has been performed. The approximate paths in stress plane are shown in Figure 3-3b and the prescribed strains are shown in Table 3-1. The stress states, based on independent computations by five groups, are tabulated in Table 3-2. Acceptable variation is considered to be $\pm 1\%$. The amount of inelasticity increases as the path number increases from 1 to 4. Thus, in path 1 (hydrostatic compression) it makes negligible difference whether large or small strain increments are used, since the response is almost linear. However, in path 4 (similar to unconfined compression) it makes considerable difference to some methods whether large or small strain increments are used, since the response is markedly nonlinear.

SUBDIVIDING STRAIN INCREMENTS (SPLITTING)

Due to the extra cost required to perform splitting, which can be a substantial increase for finite difference codes, some studies were performed to indicate the rate of consequence with number of splits or strain subdivisions. This information is summarized in Tables 3-3 through 3-5. For the present model and magnitude of strain increments it appears that less than 10 splits of the strain increment lead to acceptable conveyance. However, even 10 splits may impose an unacceptable burden on the cost of a large calculation if all strain increments for all zones are split indiscriminantly. Thus it is desirable to have an automatic procedure for determining when splitting is necessary and how many splits will lead to acceptable convergence. At present, no universally accepted criterion has been developed which applies to all situations. Criteria have been devised for individual problems, however. One of these is illustrated in Figure 3-10.

ITERATIVE TECHNIQUES

Even if the stress and strain increments are kept small, by the device of splitting, it is still likely that a stress point which should lie on the cap at the end of a subincrement does not lie on it. This happens because motion of the cap depends on plastic strain increments and is therefore not known until the end of an increment or a split. Since the motion of the cap can be of the same order as the stress increment, deviation between stress point and cap may develop. To avoid or minimize this, iteration is performed within a strain increment or split. Two types of iteration are described in Appendix A which have been used for the capped model.



TABLE 3-2. STRESS STATES CORRESPONDING TO STRAIN PATHS IN TABLE 3-1

Path 1

$$\frac{(E_1 + E_2 + E_3)/3}{(\text{in./in.})} \quad \frac{(\sigma_1 + \sigma_2 + \sigma_3)/3}{(\text{ksi})}$$

0.000238	5.00
0.00238	49.9
0.0238	498

Path 2

E_1 (in./in.)	σ_1 (ksi)	$E_2 = E_3$ (in./in.)	$\sigma_2 = \sigma_3$ (ksi)
0.00032	4.65	0.000113	3.41
0.0032	46.4	0.00113	34.0
0.032	462	0.0113	339
0.064	900	0.0226	668

Path 3

E_1 (in./in.)	σ_1 (ksi)	$E_2 = E_3$ (in./in.)	$\sigma_2 = \sigma_3$ (ksi)
0.00035	4.48	0.0000626	2.75
0.0035	44.7	0.000626	27.5
0.028	357	0.000501	2.9
0.056	670	0.01	425

Path 4

E_1 (in./in.)	σ_1 (ksi)	$E_2 = E_3$ (in./in.)	$\sigma_2 = \sigma_3$ (ksi)
0.000413	3.67	-0.0000875	0.665
0.00661	57.5	-0.0014	14.0
0.0115	99.1	-0.00245	27.0
0.0331	275	-0.00701	95.0

Path 5

E_1 (in./in.)	σ_1 (ksi)	$E_2 = E_3$ (in./in.)	$\sigma_2 = \sigma_3$ (ksi)
-0.0000496	-0.893	-0.0000348	-0.805
-0.000795	-3.0	-0.000557	-3.0



TABLE 3-3. VALUE OF HARDENING PARAMETER FOR PATH 4 (WITH CAP)
OBTAINED BY GROUP 2 FOR DIFFERENT AMOUNTS OF SPLITTING

Hardening Parameter L, ksi

Strain E_1	Strain Increment			
	ΔE	$\Delta E/10$	$\Delta E/100$	$\Delta E/1000$
0.000413	0	0	0	0
0.00661	19.2	58.7	59	58.9
0.0115	66.2	109	110	110
0.0331	409	352	359	359



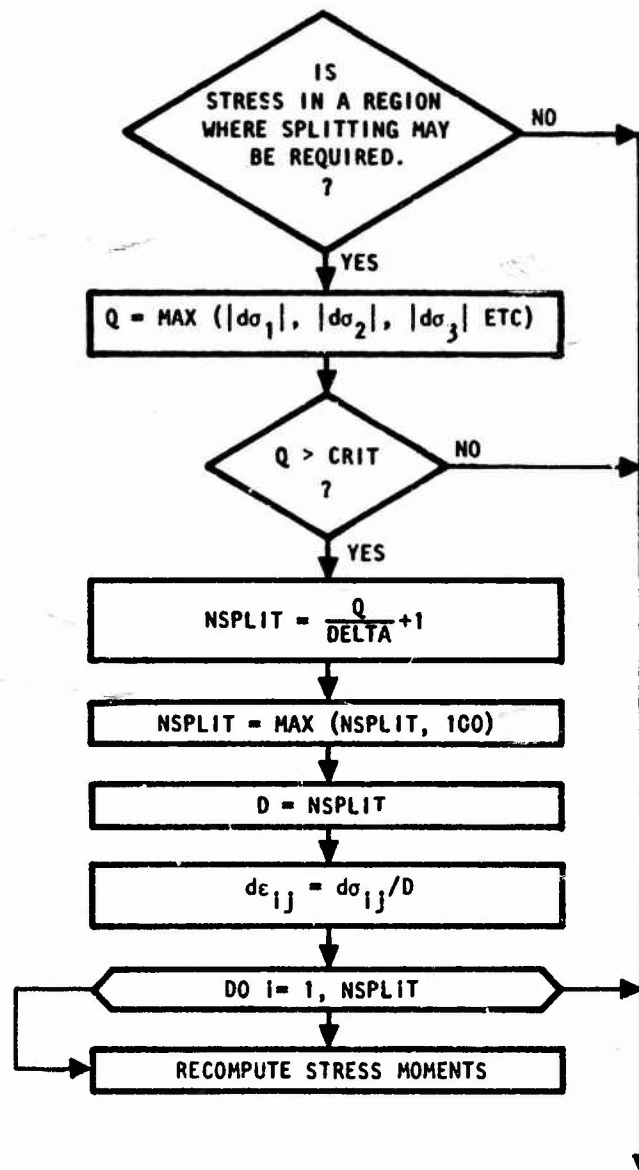
TABLE 3-4. VALUE OF AXIAL STRESS (σ_1) FOR PATH 4 (WITH CAP) OBTAINED WITH DIFFERENT AMOUNTS OF SPLITTING BY THREE GROUPS. DIFFERENCE BETWEEN GROUPS 1 AND 2 FOR $\Delta E/1000$ IS ATTRIBUTED TO DIFFERENT DEFINITION OF STRAIN VARIABLES.

Group		Axial Stress, σ_1 , ksi			
	Strain E_1	Strain Increment			
		ΔE	$\Delta E/10$	$\Delta E/100$	$\Delta E/1000$
2	0.000413	3.67	3.67	3.67	3.65
	0.00661	58.7	57.7	57.7	57.7
	0.0115	88.2	99.9	100.0	99.9
	0.0331	272	277	278	278
1		$\Delta E/N$ ($N < 100$)		$\Delta E/250$	$\Delta E/1000$
	0.000413	3.67		3.67	3.67
	0.00661	57.5		57.5	57.5
	0.0115	99.1		99.2	99.1
	0.0331	272.		273	273
		ΔE	$\Delta E/2$		
3	0.000413	3.67	3.67		
	0.00661	57.9	57.9		
	0.0115	100.7	100.6		
	0.0331	275.0	275.0		



TABLE 3-5. VALUE OF RADIAL STRESS (σ_2) FOR PATH 4 (WITH CAP) OBTAINED WITH DIFFERENT AMOUNTS OF SPLITTING BY THREE GROUPS

Group	Strain E_1	Strain Increment			
		ΔE	$\Delta E/10$	$\Delta E/100$	$\Delta E/1000$
2	0.000413	0.664	0.664	0.662	0.649
	0.00661	10.7	14.1	14.1	14.1
	0.0115	15.6	27.3	27.3	27.3
	0.0331	57.9	96.4	97.0	97.0
1		$\Delta E/N$ ($N < 100$)		$\Delta E/250$	$\Delta E/1000$
	0.000413	0.665		0.665	0.665
	0.00661	14.0		14.0	14.0
	0.0115	26.9		26.9	26.9
	0.0331	94.2		94.4	94.3
		ΔE	$\Delta E/2$		
3	0.000413	0.664	0.664		
	0.00661	13.9	13.9		
	0.0115	27.0	27.0		
	0.0331	94.5	94.5		



Main uncertainties are:

Computation of Q--individual stress components or individual strain components or frequencies thereof, such as $Q = |d\epsilon_1| + |d\epsilon_2| + |d\epsilon_3|$ are used.

Choice of CRIT--magnitude of Q which signals that a stress or strain increment large enough to require splitting has occurred.

Choice of DELTA--number of splits that are going to be allowed, up to 100 in the present example.

AA4855

FIGURE 3-10. AUTOMATIC SPLITTING



SECTION 4

SUMMARY AND CONCLUSIONS

In the present study, various methods of coding constitutive equations are examined. It is found that certain details of coding can affect the accuracy with which stresses are computed from prescribed strains and strain increments. A series of test cases, including computation of wave propagation in a split-Hopkinson bar apparatus and prescribed strain paths, is described which will help reveal coding errors in cases where complicated constitutive equations are being coded for the first time.

Specific findings of the present study include the following:

- a. Inaccuracy in computing stress from strain increments can be reduced to an acceptable level by the devices of iteration for the values of variables which are implicit functions of their arguments, such as Q in Figure 2-3, and by subdividing or 'splitting' strain increments.
- b. Iteration and splitting may increase the cost of numerical computations significantly. Hence, it is necessary to have automatic controls which introduce iteration and splitting only when necessary. Widely applicable criteria for this have not been found. Some suggestions for the specific model and stress paths considered in the present report are given above.



REFERENCES

1. Sandler, I., Letter to Mr. C. B. McFariand, Headquarters DNA, 11 March 1971.



APPENDIX A

METHODS OF CODING THE CAPPED MODEL

One iterative method involves adjusting the stresses in different ways according to whether σ_{tr} lands in Region 2 or in 3 or 4 of Figure A-1. If σ_{tr} lands in 2, the ultimate stress state is defined to be on the fracture surface. A linear approximation to the surface in the vicinity of σ_{tr} is made, and a previously derived correction formula (which uses the plastic potential flow rule) is applied to the stresses. The linear approximation is necessary, according to one group, because it is otherwise not possible to work out the correction in closed form.

If σ_{tr} lands in Region 3 or 4, the ultimate stress state is defined to be on the cap. However, at this state, the cap corresponding to the ultimate stress state has not yet been defined. Thus it is necessary to iterate for a stress state which coincides with a cap. First, a trial stress state is computed based on the position of the cap at the previous step and the plastic potential flow rule. When a cap which supposedly corresponds to the new stress state is computed, it is found that the cap and stress state do not coincide because the equations used to relate the stress state to the cap parameter are based on the assumptions of small increments. To reconcile the position of the cap to the stress state, a binary search is used.

As illustrated in Figure A-1, a temporary upper bound point on the next cap (S^+) is defined by assuming the strain increment to be entirely elastic. A temporary lower bound point on the next cap (S^-) is defined as shown. The midpoint between S^- and S^+ is adopted as a trial state on the next cap. A trial value of L and all partial derivatives are evaluated at the trial state. From these quantities, a new cap is computed. If the trial state does not lie on the cap within some tolerance, changes are made in the trial state by an iterative procedure such that the stress point eventually coincides with a cap. Similar procedures are used to determine a stress point on the fracture surface, which is an easier matter since it is stationary.

For finite element applications, it is convenient to cast the instantaneous incremental stress/strain relations in the following matrix form

$$d\sigma = C d\varepsilon \quad (A-1)$$

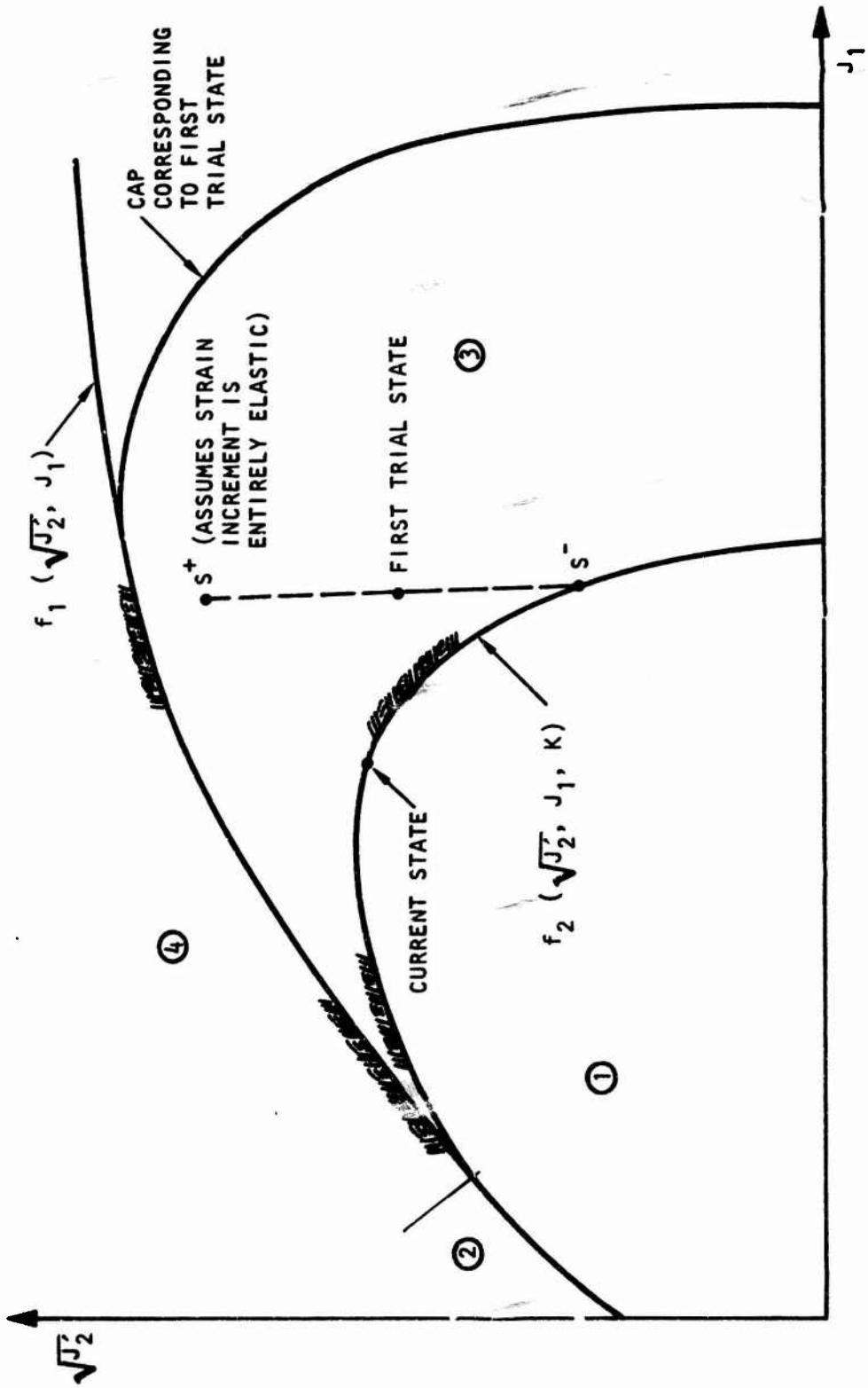


FIGURE A-1. FIRST STAGE OF ONE TYPE OF ITERATIVE TECHNIQUE



The iterative scheme shown in Figure A-2 is similar to the modified Euler formula. The procedure to obtain the stress increment during a step is described below.

$$\{\Delta\sigma\}_{k+1} = \frac{1}{2} \{ [C]_k + [C]_{k+1} \} \{\Delta\epsilon\}_{k+1} \dots \dots \dots (A-2)$$

where $[C]_k$ and $[C]_{k+1}$ are the instantaneous stress/strain relationships at the beginning and the end of the step, respectively. Since $[C]_{k+1}$ depends on the stresses at the end of the time step, successive corrections to $[C]_{k+1}$ and to $\{\Delta\sigma\}_{k+1}$ are made until the following function of stress increments reaches a stationary value within a prescribed tolerance:

$$E = |\Delta\sigma_1| + |\Delta\sigma_2| + |\Delta\sigma_3| \dots \dots \dots (A-3)$$

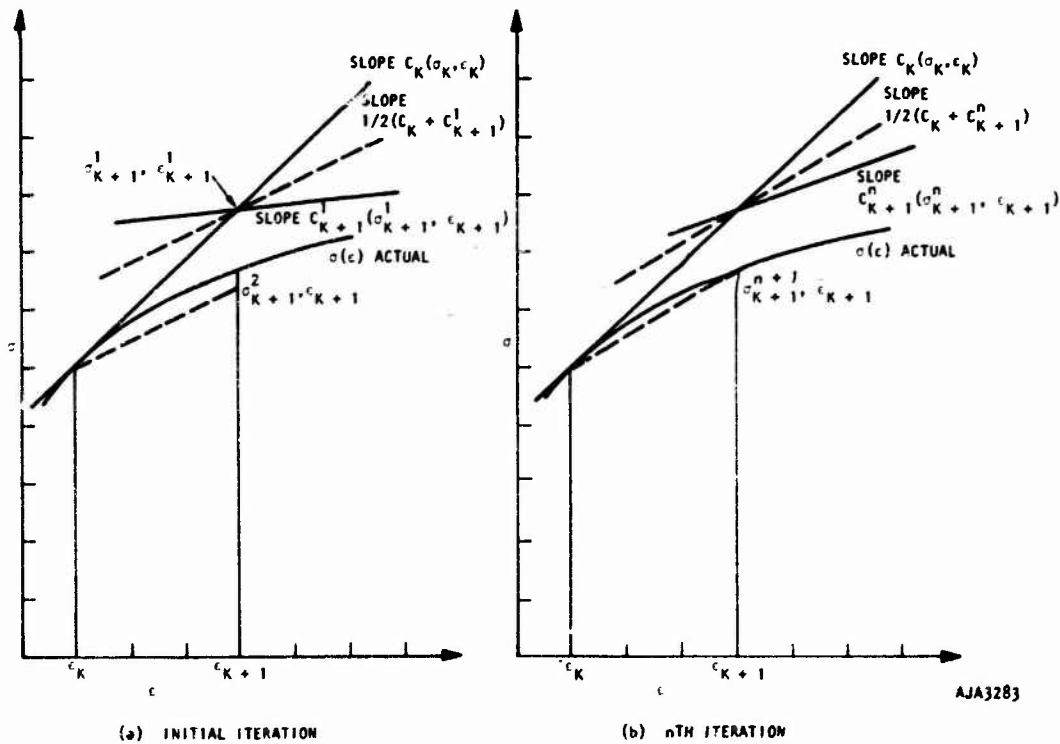


FIGURE A-2. ITERATION SCHEME TO EVALUATE STRESSES